


Article

An Application of Hyperspectral PRISMA Dataset to Characterize the Solfatara Crater, Southern Italy

Maria Pedone  and Paola Manzari * 

Agenzia Spaziale Italiana, Rome, Italy

* Correspondence: paola.manzari@asi.it

Received: 5 August 2024; **Revised:** 10 September 2024; **Accepted:** 10 October 2024; **Published:** 10 November 2024

Abstract: The Campi Flegrei area (CF) is a highly significant site for scientific investigation due to its dual importance in both Earth and Planetary Sciences. On the one hand, from a natural hazard perspective, CF is considered one of the most dangerous volcanoes on Earth because of its proximity to a densely populated urban area—the Neapolitan district, which hosts approximately three million people living between CF, Vesuvius, and Ischia. On the other hand, from a planetary science viewpoint, the high-temperature geothermal environment of the Solfatara crater serves as a terrestrial analogue to early rocky bodies within the Solar System and thus represents a prime target for astrobiological research. As part of a comprehensive site characterization, we present preliminary results using PRISMA data for the mineralogical mapping of acidic surface deposits in the Solfatara crater and the remote detection of fumarolic gases. Two PRISMA datasets were analyzed: one acquired before and one after the most significant earthquake in the area in the past 40 years, which occurred on 27 September 2023. Our initial findings reveal some variations in carbon dioxide emissions from the fumarolic field.

Keywords: Carbon Dioxide; PRISMA Mission; Remote Sensing; Campi Flegrei; Natural Hazard; Hyperspectral Analysis

1. Introduction

The Campi Flegrei area (CF) is one of the most dangerous volcanoes on Earth in terms of its proximity to a densely populated urban area [1]. The most active volcanic sites in CF are Solfatara, whose crater hosts three main high-temperature fumaroles [1–4] and Pisciarelli, a NE-SW fault-related fumarolic field located a few hundred meters east of Solfatara. Intense and persistent outgassing occurs at these fumarolic areas affecting humans, vegetation [5] and fauna. Moreover, the area is affected by widespread soil CO₂ release from “diffuse degassing structures” [6] which sustain a total CO₂ output of $\sim 1100 \pm 120 \text{ t d}^{-1}$ [4]. At Solfatara crater, fumarolic characterization was carried out by using in-situ analysis (e.g., [2]) or proximal by using Tunable Diode Laser Spectroscopy [4]. The adoption of novel technologies to estimate fumarolic CO₂ fluxes has revealed that the fumarolic contribution to the whole CO₂ flux of the area is substantial, representing $\sim 50\%$ of the soil CO₂ output [2, 4]. In a study by Pedone et al. [1], fumarolic CO₂ emissions at Campi Flegrei and their dispersion in the lowest atmospheric boundary layer were investigated, innovatively utilizing a Lagrangian Stochastic dispersion model combined with the Eulerian model (DISGAS) to diagnose the dispersion of diluted gas plumes over large and complex topographic domains. In

terms of natural hazards, the monitoring of fumarolic gases (mainly carbon dioxide) release is crucial to collect the variation of gases concentration emitted from the main vents and to understand if any volcanic activity renewal is occurring.

Moreover, in the field of Planetary Science, the minerals outstanding in the Solfatara crater may give clues about the hydrothermal processes on Mars planet since the area is considered like a Mars analog [7]. In this sense, the Solfatara crater is also an important site to investigate the mineralogical alteration processes that may have occurred in the Early Solar System and better understand the evolution of Early Mars and Early Earth.

Mineralogical studies on the Solfatara site were carried out by Caputo et al. [8], by means of optical observations, X-Ray Powder Diffractometry (XRPD), and Scanning Electron Microscopy (SEM). The authors could characterize the site as consisting of native sulfur (S), Na-alunite $\text{KAl}_3(\text{SO}_4)_2(\text{OH})_6$, mscagnite $(\text{NH}_4)_2(\text{SO}_4)_4$, amorphous silica, quartz SiO_2 , barite $\text{Ba}(\text{SO}_4)$, illite $(\text{K},\text{H}_3\text{O})(\text{Al},\text{Mg},\text{Fe})_2(\text{Si},\text{Al})_4\text{O}_{10}[(\text{OH})_2,(\text{H}_2\text{O})]$, montmorillonite $(\text{Na},\text{Ca})_{0.3}(\text{Al},\text{Mg})_2\text{Si}_4\text{O}_{10}(\text{OH})_2 \cdot n(\text{H}_2\text{O})$.

In this study, we show a comprehensive (main minerals + gas) characterization of the Solfatara crater achieved through the exploitation of hyperspectral PRISMA [9] data. Here, we aim to characterize the acidic products of the Solfatara crater floor and propose a method to analyze fumarolic carbon dioxide detection from space.

For analyzing the variation of volcanic carbon dioxide concentrations, the method, addressed in the following section, was applied to two sets of data. One dataset was acquired by PRISMA on 18th February 2021, which is before the earthquake occurred on 27th September 2023 at 1:35 UTC [10]. Instead, the second dataset was obtained by PRISMA on 27th September 2023 at 9:51 UTC, about 8 hours after the seismic event occurred.

The earthquake occurred on 27th September 2023 ($M_d = 4.2 (\pm 0.3)$ [10]) was the higher energy seismic event occurred in the last 40 years, and the major event after the brady-seismic renewal started in 2005 [10].

Our results show that a certain increase in carbon dioxide concentration could be observed before and after the main earthquake. It is noted that this is a preliminary study: in the future, a lot of measurements are necessary to achieve a correlation (if any) between the data achieved by PRISMA and the volcanic activity of the investigated area.

2. Materials and Methods

2.1. Mineralogical Characterization

To spectrally characterize the minerals occurring in the Solfatara site, we used the PRISMA L2 reflectance products. We computed the ratio between the pixel spectra in the Solfatara site and the average spectrum of the whole PRISMA product, excluding black and water related pixels.

2.2. Gas Detection

To evaluate whether the PRISMA satellite may detect CO_2 variations following tectonic-volcanic events in the Solfatara area, we compare PRISMA acquisitions pre- and post- seismic event. One PRISMA observation is collected 8 hours after the main earthquake on 27th September 2023 (**Figure 1**), and another observation is collected on 18th February 2021. The observation taken on 18th February 2021 (**Figure 2**) is already studied by Romaniello et al. [11]. The choice of selecting the same data was made to validate our method by comparing our results with results from Romaniello et al. [11].

To quantify CO_2 concentrations, we applied the Continuum Interpolated Band Ratio (CIBR [12]) technique to the two PRISMA observations. The CIBR algorithm processes radiance signals to extract CO_2 concentration information by comparing specific spectral bands. The CIBR index is defined as follows:

$$\text{CIBR} = L_c/A \times L_l + B \times L_r \quad (1)$$

where L_c is radiance at 2061 nm, L_l is radiance at 1985 nm, L_r is radiance at 2111 nm. In the context of the CIBR technique, A and B are weighting factors in Equation (1) that quantify the spectral separation between the “shoulder” wavelengths—regions of the spectrum that exhibit minimal to no gas absorption—and the wavelength of the

channel that is significantly impacted by gas absorption. A and B are coefficients that can vary but must sum up to 1. Since the range between 1900–2100 nm is also affected by absorptions related to water, Romaniello et al. [11] investigated the optimal A e B values to minimize the influence of CIBR from the water contribution.



Figure 1. RGB image (left) and zoom on Solfatara (right) of PRISMA L2 product collected on 27th September 2023. Yellow arrows indicate the Solfatara site.



Figure 2. RGB image (left) and zoom on Solfatara (right) of PRISMA L2 product collected on 18th February 2021. Yellow arrows indicate the Solfatara site.

In our work, we used $A = 0.15$ and $B = 0.85$, which resulted to be the best values for avoiding the influence of water in CIBR calculation [11].

The CIBR was calculated using Level 1 (L1) data, focusing on pixels exclusively within the Solfatara region. We used the Planetary Spectrum Generator (PSG) to simulate PRISMA radiance data with a standard atmospheric model and increasing CO_2 concentrations. The supplementary materials provide the parameters of PSG model in input. To constrain the eventual contribution of fumarolic CO_2 , simulations were computed starting from a standard atmospheric CO_2 concentration of 400 ppm (local background; [4]).

We computed the CIBR using data from the PSG simulation of the PRISMA observations with increasing concentrations (in ppm): 400, 600, 800, 1000, 1500 (**Table 1**). **Table 1** shows the parameters in input for the simulations on the two observations.

Table 1. Input parameters used in the PSG simulations on 18 February 2021 and 27 September 2023.

Input Parameter	Value	Note
Spectral range	0.35–2.55 μm	Spectral range of detection of PRISMA satellite
Atmospheric profiles	US standard 1976	Reference atmospheric model
Surface temperature	(US standard 1976) 290 K	
CO_2 concentrations	400, 600, 800, 1000, 1500 ppm	See text
Ground reflectance	0.10	Reflectance value at surface
Altitude of the first layer	0 km	First layer of the model US standard 1976
Altitude of the last layer	120 km	
Number of vertical levels	53	
Aerosol	NO	
Composition of the ground	70% Clays	Abundance of clays respect to other minerals found by XRD
H_2O column amounts	1.416 g/cm^3	Vapor water in atmosphere

3. Results

By using PRISMA L2 products we could remotely identify overall features around 2.2 micrometers. Among the minerals that feature absorptions around 2.2 micrometers we found a similarity in the shape with the spectral absorptions of gypsum, alunite, and illite-montmorillonite, from the USGS library (**Figure 3**).

Concerning the gas detection, at first, we simulated also the observation of 18th February 2021, getting the CIBR values corresponding to simulated concentrations (ppm): 400, 600, 800, 1000, 1500 (**Figure 4**).

The mathematical relation between CIBR and concentrations resulted better approximated by a polynomial quadratic curve as it can be observed from the plot of CIBR variations in relation to the background concentration, 400 ppm (**Figure 5**, blue points).

Then, we plot the mean CIBR computed on real PRISMA observation related to 18th February 2021, to get the corresponding value of concentration. It resulted in about 600 ppm (**Figure 5**, orange point).

The choice to extract the mean CIBR only on those pixel spectra within the Solfatara was made to reduce the effects of local noise in the signal data and therefore to keep a conservative approach.

Then we simulated also the observation of 27th September 2023, getting the CIBR values corresponding to simulated concentrations (ppm): 400, 600, 800, 1000, 1500 (**Figure 6**).

Also, in this case, the mathematical relation between CIBR and concentrations resulted better approximated by a polynomial quadratic curve as it can be observed from the plot of CIBR variations in relation to the background concentration, 400 ppm (**Figure 7**, blue points). As in the case of 18th February 2021, we plot the mean CIBR computed on the pixel spectra within the Solfatara from the PRISMA observation related to 27th September 2023. The corresponding value of concentration resulted in about 750 ppm, as shown in **Figure 7** (orange point).

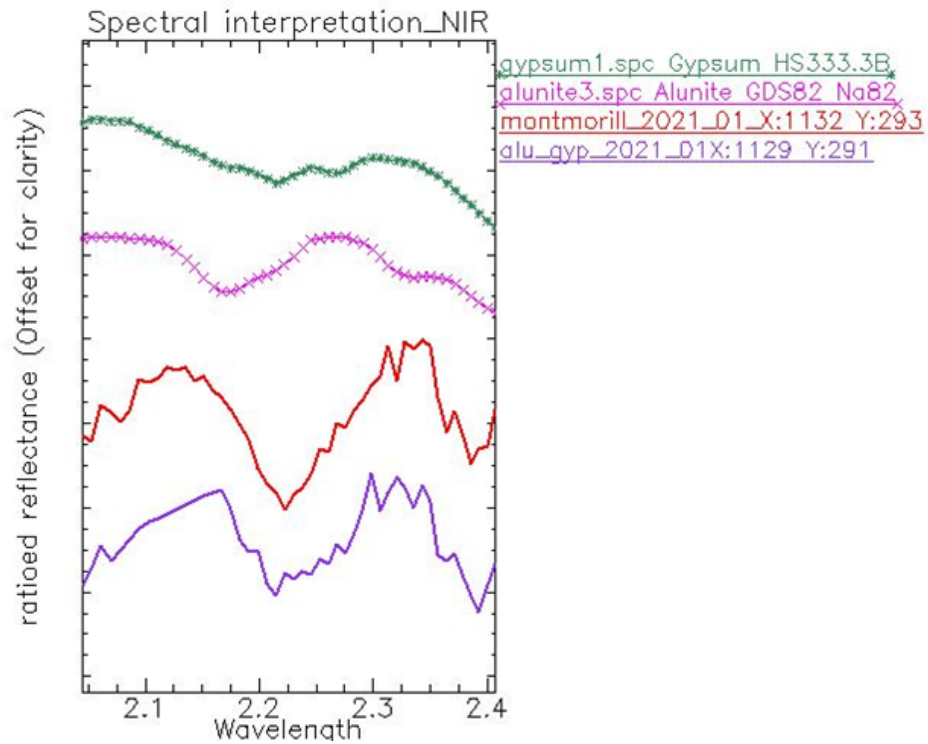


Figure 3. Solid lines= spectral absorptions in PRISMA spectra on the Solfatara site; dotted lines = reference spectra from USGS library.

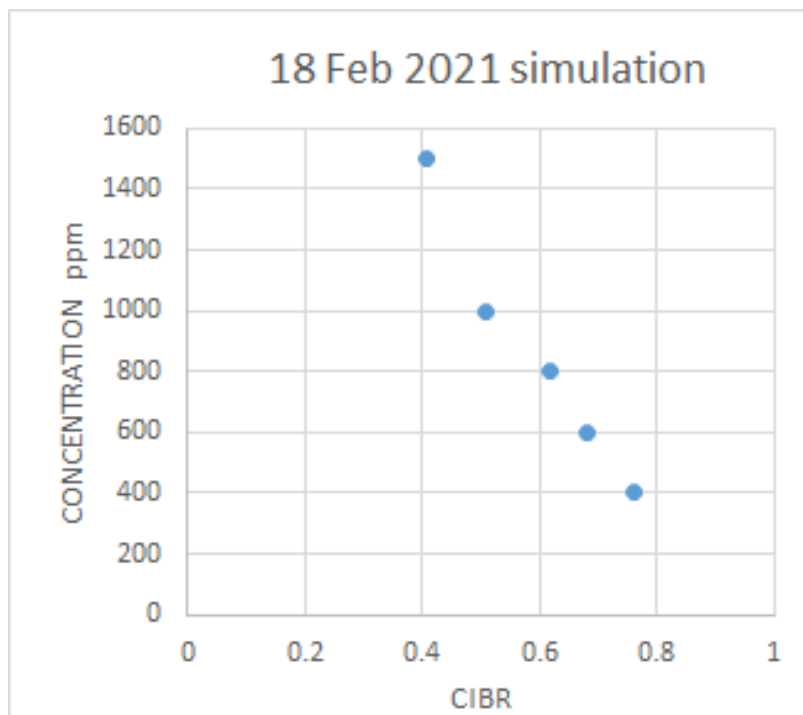


Figure 4. PSG simulations of CO₂ different concentrations on PRISMA observation collected on 18th February 2021 on Solfatara.

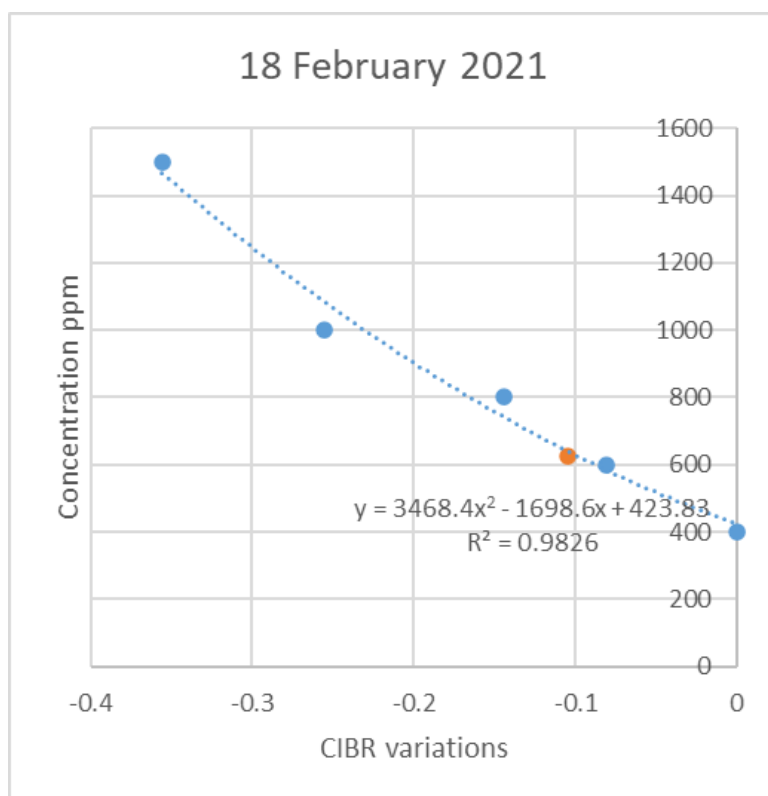


Figure 5. Plot of CIBR variations respect to 400 ppm background CO₂ vs. corresponding simulated concentrations. Blue series are CIBR from simulated data, orange point is CIBR obtained from the real PRISMA observation. The error on the real CIBR value is 10%.

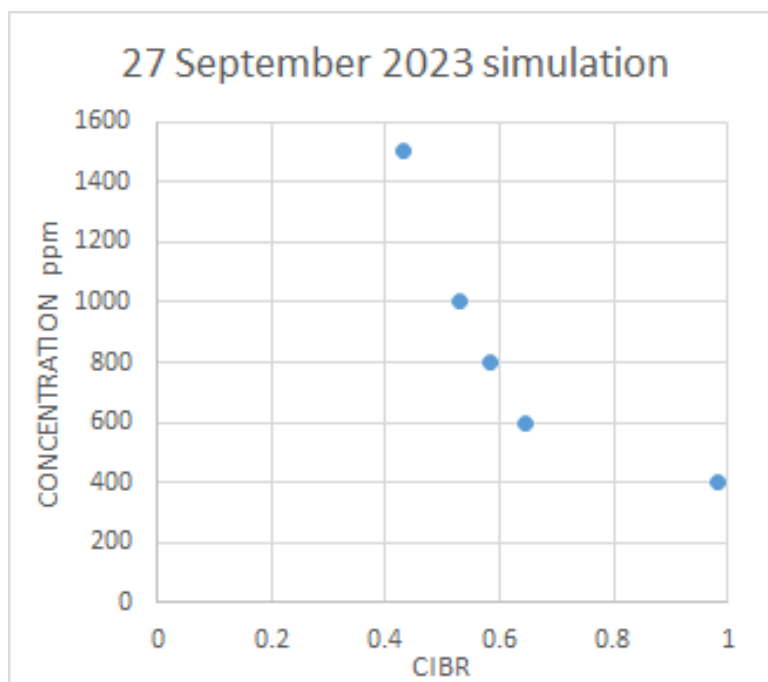


Figure 6. PSG simulations of CO₂ different concentrations on PRISMA observation collected on 27th September 2023 on Solfatara.

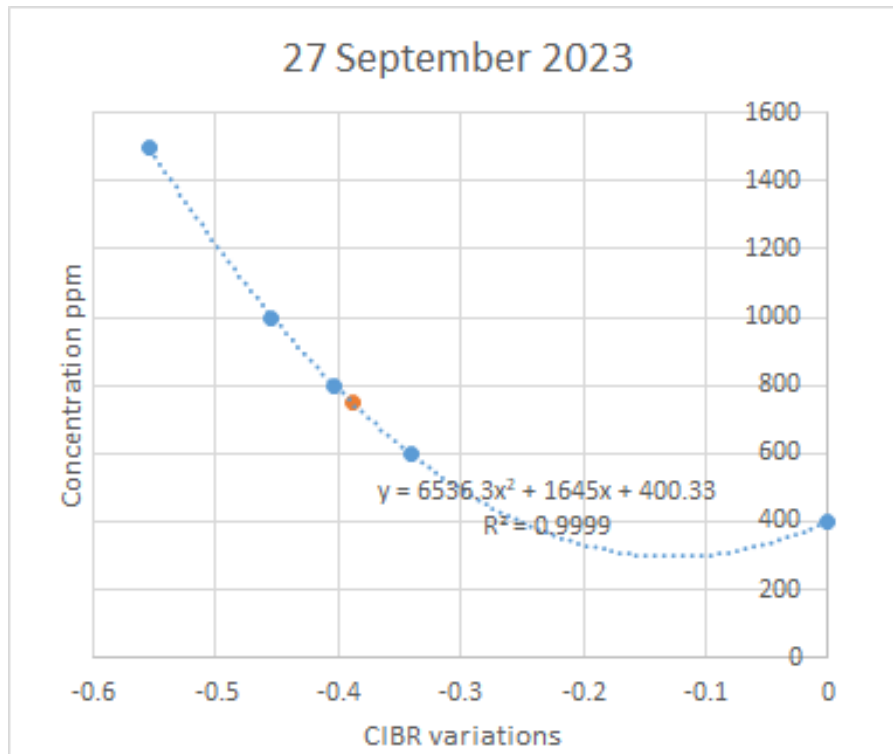


Figure 7. Plot of CIBR variations respect to 400 ppm background CO₂ vs. corresponding simulated concentrations. Blue series are CIBR from simulated data, orange point is CIBR obtained from the real PRISMA observation. The error on the real CIBR value is 10%.

4. Discussion and Conclusions

The central target addressed in this study is how hyperspectral data from the PRISMA mission [9] can be used to characterize both the mineralogical composition of the Solfatara crater and variations in fumarolic carbon dioxide (CO₂) emissions following seismic events. Specifically, this work explores whether the PRISMA hyperspectral dataset can be used to detect CO₂ concentration variations associated with tectonic-volcanic activity, especially in the context of a major seismic event that occurred on 27th September 2023.

This study fills a significant gap by applying remote sensing for both geological and atmospheric characterization of a hazardous volcanic site. This is particularly critical for densely populated regions like Campi Flegrei.

Moreover, by linking the findings to planetary science (Mars analog studies), our research broadens its relevance beyond Earth sciences to astrobiology and planetary exploration.

Concerning the mineralogical characterization of the Solfatara site, by using PRISMA hyperspectral data we may confirm the occurrence of the main absorptions related to a mixing of sulphates, illite and montmorillonite, as main minerals remotely detectable. This finding agrees with the mineralogical composition of samples collected in the Solfatara site by Caputo et al. [8].

In this view, the Solfatara site could represent a potential analogue site [7] for the study of Mars-like environments with geological evidence of past volcanic activity and/or where the same mineralogical associations occur (**Figure 8**). In particular, PRISMA hyperspectral data in this area can be used to interpret data collected by the Compact Reconnaissance Imaging Spectrometer for Mars (CRISM) onboard the Mars Reconnaissance Orbiter (MRO) [13, 14] and references therein. For example, the alunite mineral was identified in the CRISM spectra on Cross crater, in the area of Terra Sirenum, indicating acidic environment, like in the case of Solfatara, characterized by sulfurous waters in that area in the past, possibly linked to magmatic activity [15].

Concerning volcanic gas emissions, since the unrest period started in 2005, the area of Solfatara recorded an increase of fumarolic $\text{CO}_2/\text{H}_2\text{O}$ ratio (from 0.2 before the unrest to 0.40 at present), underling an increase of hydrothermal input in the volcanic conduit [10]. Also, the total CO_2 flux from the entire area (Solfatara + Pisciarelli) increased from 3200 t/d (in 2020) to 4000 t/d (in 2023) [10]. The unrest started in 2005 was accompanied by seismicity in the area with 2 main high energy earthquakes: one on 27th September 2023 ($M_d = 4.2$) and on 20th May 2024 ($M_d = 4.4$; the latter not discussed in this study). Our work aims to use the CIBR-based model [11, 12] to derive the CO_2 concentrations emitted from the fumarolic field of Solfatara and find (if any) variations of CO_2 concentrations in the two PRISMA datasets (in 2021 and in 2023). Our work shows an average variation in the concentration of (emitted) CO_2 of 150 ppm between the observation related to 18th February 2021 and the other related to 27th September 2023. This concentration increment could be (or not) related to an increase of hydrothermal gases input after the earthquake of 27th September 2023. We are not able to compare our PRISMA-based results with direct CO_2 measurements in the fumaroles, on the same day (a special permission is needed to enter and take in-situ samples/measurements for surveillance since the end of 2017). However, we can refer to the seismicity/volcanology information that is freely available in the INGV bulletin [10]. We found that a fixed station installed at Pisciarelli, at higher level to respect the level of the fumaroles, measured in-air- CO_2 concentrations of 2500–3000 ppm in 2021 and 3500 ppm in September (and October) 2023 [10]. In other words, our 150-ppm increment from 2021 to 2023 (our study) could be related to about 500–1000-ppm increment measured from the fixed in-air-station. We would emphasize that this is preliminary pioneering research since hyperspectral analysis is new and under development yet. We support the idea that long temporal series are necessary to find (if any) correlation between proximal (ground stations) and remote (from satellites) signals. A more adequate hyperspectral dataset is necessary to have a robust statistical analysis.

At present, this study demonstrates how hyperspectral data can supplement and extend the previous well-known in-situ techniques applied to volcanic hazard assessment, offering continuous wide-area coverage.

This study demonstrates the potential of remote sensing to monitor volcanic emissions at a regional scale and leverages remote sensing to expand the accessibility of volcanic monitoring.

Author Contributions

M.P. designed this study, wrote the manuscript and discussed the results. P.M. analyzed PRISMA datasets, validated the CIBR-method, and carried out the simulations. All authors have read and agreed to the published version of the manuscript.

Funding

This work received no external funding.

Institutional Review Board Statement

Not applicable.

Informed Consent Statement

Not applicable.

Data Availability Statement

PRISMA data used in this work are available at URL: <http://prisma.asi.it/>.

Acknowledgments

This study was supported by the Directorate of Science and Innovation of ASI. This work benefits from two anonymous reviewers' comments useful to improve the previous version.

Conflicts of Interest

The authors declare no conflict of interest.

References

1. Pedone, M.; Granieri, D.; Moretti, R.; et al. Improved quantification of CO₂ emission at Campi Flegrei by combined Lagrangian Stochastic and Eulerian dispersion modelling. *Atmos. Environ.* **2017**, *170*, 1–11.
2. Aiuppa, A.; Tamburello, G.; Di Napoli, R.; et al. First observation of the fumarolic gas output from a restless caldera: implications for the current (2005–2013) Campi Flegrei unrest. *Geochem. Geophys. Geosyst.* **2013**, *14*, 4153–4169.
3. Fedele, A.; Pedone, M.; Moretti, R.; et al. Real-time quadrupole mass spectrometry of hydrothermal gases from the unstable Pisciarelli fumaroles (Campi Flegrei): Trends, challenges and processes. *Int. J. Mass Spectrom.* **2017**, *415*, 44–54.
4. Pedone, M.; Aiuppa, A.; Giudice, G.; et al. Volcanic CO₂ flux measurement at Campi Flegrei by tunable diode laser absorption spectroscopy. *Bull. Volcanol.* **2014**. [CrossRef]
5. Bartiromo, A.; Guignard, G.; Barone Lumaga, M.R.; et al. Influence of volcanic gases on the epidermis of *Pinus halepensis* Mill. in Campi Flegrei, Southern Italy: a possible tool for detecting volcanism in present and past floras. *J. Volcanol. Geotherm. Res.* **2012**, *233–234*, 1–17.
6. Chiodini, G.; Frondini, F.; Cardellini, C.; et al. CO₂ degassing and energy release at Solfatara volcano, Campi Flegrei, Italy. *J. Geophys. Res.* **2001**, *106*, 16213–16221.
7. Flahaut, J.; Bishop, J.L.; Silvestro, S.; et al. The Italian Solfatara as an analog for Mars fumarolic alteration. *Am. Mineral.* **2019**, *104*, 1565–1577.
8. Caputo, T.; Mormone, A.; Marino, E.; et al. Remote Sensing and Mineralogical Analyses: A First Application to the Highly Active Hydrothermal Discharge Area of Pisciarelli in the Campi Flegrei Volcanic Field (Italy). *Remote Sens.* **2022**, *14*, 3526.
9. Caporusso, G.; Lopinto, E.; Lorusso, R.; et al. The Hyperspectral Prisma Mission in Operations. In Proceedings of the IEEE International Geoscience and Remote Sensing Symposium, Waikoloa, HI, USA, 26 September–2 October 2020; pp. 3282–3285. [CrossRef]
10. INGV - Osservatorio Vesuviano Bulletin. Available online: <https://www.ov.ingv.it/index.php/monitoraggio-e-infrastrutture/bollettini-tutti/mensili-dei-vulcani-della-campania/flegrei/anno-2023-1> (accessed on September 2023).
11. Romaniello, V.; Spinetti, C.; Silvestri, M.; et al. A Methodology for CO₂ Retrieval Applied to Hyperspectral PRISMA Data. *Remote Sens.* **2021**, *13*, 4502.
12. Amici, S.; Piscini, A. Exploring PRISMA Scene for Fire Detection: Case Study of 2019 Bushfires in Ben Halls Gap National Park, NSW, Australia. *Remote Sens.* **2021**, *13*, 1410.
13. Murchie, S.; Arvidson, R.; Bedini, P.; et al. Compact reconnaissance imaging spectrometer for Mars (CRISM) on Mars reconnaissance orbiter (MRO). *J. Geophys. Res. Planets* **2007**, *112*(E5).
14. Seelos, F.P.; Seelos, K.D.; Murchie, S.L.; et al. The CRISM investigation in Mars orbit: Overview, history, and delivered data products. *Icarus* **2024**, *419*, 115612. [CrossRef]
15. Ehlmann, B.L.; Swayze, G.A.; Milliken, R.E.; et al. Discovery of alunite in Cross crater, Terra Sirenum, Mars: evidence for acidic, sulfurous waters. *Am. Mineral.* **2016**, *101*, 1527–1542.



Copyright © 2024 by the author(s). Published by UK Scientific Publishing Limited. This is an open access article under the Creative Commons Attribution (CC BY) license (<https://creativecommons.org/licenses/by/4.0/>).

Publisher's Note: The views, opinions, and information presented in all publications are the sole responsibility of the respective authors and contributors, and do not necessarily reflect the views of UK Scientific Publishing Limited and/or its editors. UK Scientific Publishing Limited and/or its editors hereby disclaim any liability for any harm or damage to individuals or property arising from the implementation of ideas, methods, instructions, or products mentioned in the content.